Development and Performance Evaluation of a Steady-State Virtual Sensor for Predicting Wall Surface Temperature in Light Commercial Buildings with an Open Space

Denchai Woradechjumroen*, Haorong Li and Yuebin Yu
Durham School of Architectural Engineering and Construction, University of Nebraska-Lincoln, Omaha, NE 68588, USA.

Abstract

Multi-zone layout is commonly designed for low-rise cubicle offices or big-box retail stores. These buildings are served by multiple rooftop units (RTUs) to supply heating and cooling. Regarding this open space layout without interior walls between zones, heat balance effect between a zone and adjacent zones is occurred rather than general multi-zones with interior walls. This effect probably causes simultaneous cooling and heating or cooling fighting because each RTU has individual and uncoordinated control resulting in excessive energy use and shorter cycling operations of RTUs. To measure this effect and solve the problem, this article proposes a virtual sensor for predicting wall surface temperature by using a steady-state equation based on multiple linear regressions (MLR). Utilizing rich data of practical operations obtained from the simulation of multiple RTUs, MLR can be used to accurately extrapolate within the range of the training data. Using the building simulation platform based on heat, air and Moisture laboratory (Hamlab) without RTU operations, this simulated data are used to validate the developed model. To further evaluate the model performance, the three control modes of the multiple RTUs including undersized, right-sized and oversized capacities of multiple RTUs are simulated and studied. The results show that the proposed virtual sensor improves the implementation performances of dynamic virtual wall surface temperature sensor under off-control conditions around 16 to 20% based on goodness of fit (G). In addition, the proposed method can be applied as a tool in predicting wall surface temperatures of special cooling and heating wall in renewable energy areas.

* Corresponding author.
E-mail: dworadechjumroe@unomaha.edu

1. Introduction

According to U.S. Commercial Sector Primary Energy in 2006 (DOE, 2011), heating, ventilation, air-conditioning and refrigeration systems (HVAC & R) accounted for about 50% of the total energy used in commercial buildings. Approximately, 30% of the total energy was consumed on space cooling and space heating by HVAC systems and the rest was belong to refrigeration systems. About 62% of the total energy providing for the floor space was served by rooftop units (RTUs) for commercial buildings in the U.S. In addition, RTUs accounted for 50% of total energy used for small commercial offices and retail stores (Rivers, n.d.). One of major excessive energy uses is inherent oversizing effect in RTUs. Based on the field data analysis of 268 RTUs in 12 retail stores located in different climate regions in USA, Woradechjumroen et al. (2014) stated that the oversized RTUs has an average value of 84% for cooling and 299% for heating. These situations lead to the highest peak energy penalty that goes to 226 kW in a cooling mode and 1,375 kW in a heating mode. This oversizing problem leads to short product lifecycle due to short on-off cycling of RTU compressors and fans. Additionally, with non-synchronous control of RTUs, simultaneous cooling and heating or cooling fighting will increase more frequent compressor operations caused by uncontrolled cooling or heating effect from adjacent zones. Measuring and investigating this effect can be used to reduce cooling or heating building load for decreasing excessive energy uses and extending RTU lifecycle.

To solve the cooling fighting caused by non-coordination control of multiple RTUs, wall surface temperature between two zones can be utilized to observe this effect through estimating heat transfer interaction in light commercial buildings with an open space. The wall surface temperature can examine heat direction, and quantity of heat transfer between two adjacent zones. However, the open space is not included interior wall between zones. As a result, the physical sensors are inconveniently installed in these surroundings. Replacing the physical sensors, virtual sensors having been continuously developed in many areas such as HVAC and automotive areas can be applied to address this challenge. The concepts of virtual sensors can be categorized in three criteria (Li, Yu & Braun, 2011): measurement characteristics-based criterion (transient-state and steady-state data-based approach); modeling method-based criterion (white-box, gray-box and black-box models) and application purposes-based criterion (replacement and observing). For first criterion, steady-state based approach is typically applied to quickly modeled process from changed inputs or slowly changed

inputs of a system, so it is suitable for fault detection and diagnosis, which is theoretically desirable to quasi-static process.

For example in steady-state based criterion, Li and Bruan (2007a and 2007b) developed 11 virtual sensors based on steady-state measurement data by using low-cost temperature sensors and manufactures' rating data for applying to automated fault detection and diagnosis (AFDD) on RTUs. All developed virtual technologies were defined from white-box (first-principle) and gray-box models. In contrast to steady-state method, the transient-state based approach using a transient model to predict an immeasurable variable is typically appropriate for real-time feedback control or transient document used in AFDD. With these behaviors, fast system responses such as chemistry field (Bonne & Jorgensen, 2004) and food process (James, Legge & Budman, 2002) have applied transient virtual sensors to detect fast system changes due to existing faults in AFDD and to measure cost-effective values for a feedback control system.

With the virtual sensor backgrounds and applications, our team (Yu, Woradechjumroen & Yu, 2014) developed a virtual wall surface temperature sensor utilizing a dynamic thermal model and system identification techniques in terms of a simplified physical-based linear parametric model, as demonstrated in Appendix C. This developed virtual sensor performs well in thermal model predictions by using system identification toolbox in Matlab software. It can be used to estimate accurate temperature prediction up to 95% based on goodness of fit (G) for off-control conditions, and there are some existing errors up to 20% when it is used to predict wall surface temperatures under on-control conditions. The prediction performances are varied depending on oversizing level. Furthermore, when the sensor is implemented on Simulink in terms of state-space equations on Simulink, the model accuracy is reduced to around 70% because a loss function is caused by model transformation from discrete time to continuous time for Simulink implementation. The loss function could result in unstable response. To protect and guarantee stable response of real-time implementation, the present article applies multiple linear regressions (MLR) to generate a steady-state model of the virtual wall surface temperature sensor by using rich data obtained from a building simulation platform, which is developed from further developed based on heat, air and Moisture laboratory (Hamlab) in order to be conveniently complied on Simulink environment. The main advantages of MLR are: 1) potential and accurate for predicting and extrapolating system performances within the range of obtained data; 2) easy-to-implement for

real-time control and AFDD and 3) to guarantee stable system prediction. In this article, statistical theories are applied to systematically develop the steady-state virtual sensor to predict wall surface temperature in an open-space light commercial building such as retail stores. Results are validated by G and coefficient of determination (R^2) when off-control conditions are utilized to test in three zones. Additionally, the proposed model will be further tested with three on-control conditions to evaluate performance limitations for a future research. With the contribution, it can be applied as a tool in predicting wall surface temperatures of special cooling and heating wall in renewable energy areas.

The study is organized as follows: the knowledge and backgrounds of RTU operations including an building example and statistical theories are briefly described at first. Secondly, the steady-state model of the virtual sensor is developed based on the procedures of MLR. Then, the validation of the model will be processed through simulated data obtained from the building simulation platform utilizing the off-control condition of each RTU. To test the robustness and performance of the developed model, the sensitivity analysis of the virtual wall surface temperature model will be conducted through the three on-control conditions: proper-sized, oversized and undersized capacities, which will be applied in supervisory or coordination control of multiple RTUs. Finally, the performance of the steady-state model is concluded for contributions in a future research.
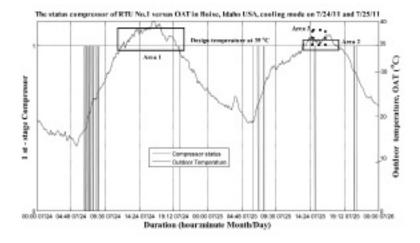
2. Backgrounds

This section briefly introduces the significant backgrounds to develop a steady-state virtual sensor for predicting wall surface temperatures in light commercial buildings. Regarding RTU routine operations, a cooling and heating mode are supplied by a RTU per zone. The thermostat of a RTU controls room temperatures by using on-off control action. Especially, undersized, right-sized and oversized capacities of multiple RTUs will be simulated for model

evaluation. This section firstly explains zone temperature effect under these three on-control conditions. After that, a building example simulated via Hamlab on Simulink is introduced with the definition of a virtual wall surface temperature. To conduct a model, statistical theories associating with multiple linear regressions (MLR) are systematically described to characterize the linear relation between independent variables and a dependent parameter.

2.1 On-off control action of a cooling mode in a rooftop unit

For the signature of oversizing analysis (Woradechjumroen et al., 2014), annual outdoor temperature designs recommended by ASHARE Handbook - Fundamentals (American Society of Heating, Referigeration and Air-Conditioning Engineering [ASHRAE], 2009) are used to separate peak design conditions from off-design conditions. For a heating mode in a RTU or heat pump, the annual heating design condition at 99% DB (dry-bulb) of each location is utilized for the oversizing analysis, whereas the annual cooling design condition at 1% DB is selected to consider the quantification of oversizing through the on/off status data of compressors for a cooling mode of the vapor compression cycle in an air-conditioning unit and heat pump.

Figure 1. Example of a propersized RTU compressor, No.1 in Idaho, USA.

In Figure 1, the one-stage compressor was recorded in Boise, Idaho USA. The annual design condition of cooling load at 1% DB is 35°C; outdoor air temperature (T_{OAT}) was higher than this temperature value, which was used to identify the peak conditions of the compressor. Area 1 and 2 showed the ranges of outdoor temperatures that were higher than the design temperature on 7/24, 2011 and 7/25, 2011, respectively. These two areas are marked out to explain the propersizing operations of the compressor that run continuously without cycling during these periods; the on-status compressor was continuously activated until the zone temperatures were out of selected operating differential range on a thermostat. This action leads to a graphically right-sizing signature of a RTU or heat pump. However, there was one cycle occurred during the peak design conditions on 7/25, 2011 in Area 2 because the compressor operation was fluctuated by T_{OAT} variation as shown in Area 3.

Figure 2. Example of an oversized RTU compressor, No.5 in Idaho, USA.

Conversely, for the same day but with the different RTU, No.5, Figure 5 illustrates the operation of an oversized first-stage compressor in a cooling mode. Comparing Figure 2 with Figure 1 for the same period on 7/25, 2011, it can be seen that the compressor cycles more frequently at the peak design temperature, 35°C, in Area 4; this happen can be regarded as the signature of oversizing. Meanwhile, the compressor statuses of undersized RTUs perform similarly to proper-sized RTU; however, a zone temperature cannot be controlled within the selected operating differential range.

2.2 Building example for testing the virtual sensor

The analysis also utilizes the same building as the proposed dynamic virtual sensor (Yu, Woradechjomroen & Yu, 2014) for comparing results. The building simulation platform using an artificial weather in Miami, Florida USA is the example for studying a small retail store in the present study, as d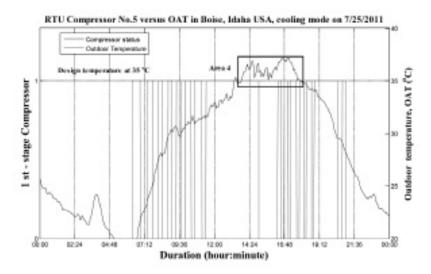epicted in Figure 3; its zones are divided into three zones with very thin interior wall using light concrete (thick = 1 mm.) between zones. The interior walls are not existed in real stores called virtual interior walls, but they are simulated by the very thin wall in the simulation for generating heat transfer from a zone to adjacent zones through the virtual walls. This building is simulated by Hamlab (Schijndel, 2007) running on Simulink in Matlab environment.

The building composes of only a concrete ground floor and a flat roof. The height of the building is 3.50 m. and all windows are assigned to be of 1.2 m. height. It has been supplied heating and cooling to the space by three one-stage RTUs installed on the roof. In addition, the routine operations, building components and internal loads are given and tabulated in Table 4 and 5 in Appendix A. The cooling model is operated by a vapor compression cycle, as depicted in Figure 3. The rated cooling capacities are 5kW., 5kW., and 6.5kW. for RTU1, RTU2 and RTU3, respectively.

In Figure 3, the simulation is assumed as follows:

1) Each zone air is perfectly mixed. As a result, it has one uniform zone temperature. This is a common approximation assumed in thermal models.

2) One wall surface temperature is equally approximated for four walls in a zone because integrating sphere approximation is used to eliminate the restriction of any geometrical from in each room for calculating radiation through building envelops. Consequently, it is possible to obtain one radiant temperature for all walls in a zone. This radian temperature is equal to wall surface temperature.

3) Each zone is defined by an area served by the RTU;

4) T_{S1}, T_{S2} and T_{S3} are defined for the three temperature interactions around the virtual interior wall between zone 1 and 2, between zone 2 and 3 and between zone 1 and 3, respectively. Each interaction shows heat transfer from the surrounding around the virtual wall surface of a current zone to the surrounding around the virtual wall surface of an adjacent zone. For instance, T_{S1} is the wall surface temperature caused by the heat transfer interaction at the virtual wall surface between zone 1 and zone 2. T_{S1} can be used to notice heat interaction between zone 1 and zone 2 without using temperature distribution profile from the center zone temperature of zone 1 (T_{Z1}) to the center zone temperature of zone 2 (T_{Z2}). In addition, the heat transfer direction from T_{Z1} to T_{S1} and the heat transfer direction from T_{Z2} to T_{S1} can be used to analyze simultaneous cooling and heating.

5) The simulated data used for the current study are three zone temperatures and three wall surface temperatures.

2.3 Statistical procedures
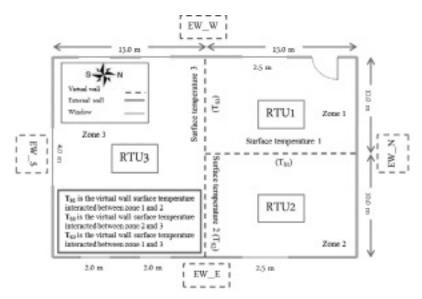The procedures of significantly statistical theories in the current study are described as follows:

Figure 3. Three-zone one-story commercial building.

1. Investigating independency between any independent variables (T_{OAT} and zone temperatures) using R^2 and tolerance values with significance., If the tolerance value is lower than 0.10, an independent variable strongly influence another independent variable (Hair, Anderson, Tatham & Black, 1995). Thus, the pair of the variable cannot be utilized to generate a MLR equation.

2. Checking a dependent variable (wall surface temperature) depending upon at least one independent variable tested by one-way analysis of variance (ANOVA) with significance (α). The relation between ANOVA and t is given by $F = t^2$. The null hypothesis (H_0) and alternative hypothesis (H_a) are listed as follows:

H_0: the independent variable ($X_i = T_{OAT}$ and zone temperatures) do not influence on a dependent variable (Y = wall surface temperature) or $\beta_i = 0$;

H_a: the independent variable ($X_i = T_{OAT}$ and zone temperatures) influences a dependent variable (Y = wall surface temperature) or $\beta_i \neq 0$;

,where i= a number of independent variables, n = the total sample size and k = the number of group levels. To further analyze, if the absolute of a calculated t-test value, $|t| > t_{1-\alpha/2;n-k-1}$ (critical value at α and degree of freedom at *n-k-1*) or a calculated F-test value, $F > F_{\alpha;k-1,n-k}$ (critical value at α and degree of freedom at *k-1* and *n-k*), the analysis refuses H_0. Otherwise, the analysis accepts H_a that concludes X impacting on the variation of Y.

3. Examining the influence of each selected independent variables on a dependent variable via t-statistic value or F test with significance

4. Computing the degree of relation between X and Y in terms of R^2 with significance, every value of X_i is associated with a value of Y. The equation is typically descript in this study as follow:

$$Y = A_0 + A_1 X_1 + A_2 X_2 + A_3 X_3 + e \quad (1)$$

Whereas e is the error at 5% out of 95% confidence of this fitting curve utilized in the study, A_0, A_1, A_2 and A_3 are constant coefficient of curve fitting from the observed data. The accurately predicted model in equation 1 is evaluated by R^2.

5. Checking conditions of a MLR equation includes:
1) constant standardized residual and
2) the error distribution is under normalcurve.

3. Steady-state model development

The concepts of virtual sensors can be categorized in the three criteria (Li, Yu & Braun, 2011): measurement characteristics-based criterion (transient-state and steady-state data-based approach); modeling method-based criterion (white-box, gray-box and black-box models) and application purposes-based criterion (replacement and observing). In this section, the proposed model is based on black-box models using MLR method in the form of a steady-state model , which does not change with time. Thus, MLR could obtain better prediction than dynamic pattern when sensitivity occurs in the system.

Table 1. Independency investigation between each independent.

Tolerance (1-R^2)	T_{OAT}	T_{Z1}	T_{Z2}	T_{Z3}
T_{OAT}	0.00	0.55	0.57	0.59
T_{Z1}	0.55	0.00	0.18	0.0004
T_{Z2}	0.57	0.18	0.00	0.20
T_{Z3}	0.59	0.0004	0.20	0.00

MLR has been intensively applied in HVAC areas, especially in AFDD applications (Yang et al., 2014; Reddy, 2006) and the prediction of building energy consumption (e.g., Aranda et al., 2012; Lam, Wan, Liu & Tsang, 2010; Catalina, Virgone & Blanco, 2008; Katipamula, Reddy & Claridege, 1998). MLR is used to model the relationship between two or more independent variables and a response variable by fitting a linear equation to observed data.

The application example of the procedures is systematically conducted in zone 1 via off-control conditions. The off-control conditions obtained from the simulation of the building using the artificial data of typical meteorological year (TMY3) T_{OAT} data sets (Wilcox & Marion, 2008) are tested by two days for peak cooling demand in July.

First of all, the first step is conducted for checking the independency of a pair of independent variables. Regarding Table 1, we will consider the three significantly independent variables including zone temperature 1 (T_{Z1}), zone temperature 2 (T_{Z2}) and outdoor air temperature (T_{OAT}) since the tolerance value between T_{Z1} and zone temperature 3 (T_{Z3}) equalling to 0.004 is less than 0.1 showing high independency. Thus, one of them, T_{Z1} is selected for the analysis.

In the second step, one-way ANOVA is used to examine the process that there is at least one independent variable strongly influencing on the dependent variable with significance. The independent variable is wall surface temperature in zone 1 (T_{S1}). The assumption is shown below:

H_0: the independent variable (T_{OAT}, T_{Z1} or T_{Z2}) does not influence on the dependent variable (T_{S1}) or $\beta i = 0$;

H_a: the independent variable (T_{OAT}, T_{Z1} or T_{Z2}) influences on the dependent variable (T_{S1}) or $\beta i \neq 0$

Using statistical toolbox in Matlab, the results of one-way ANOVA are demonstrated in Table 2.

	df (degree of freedom)	SS (sum of squares)	MS (mean square)	F	Significance
Regression	3	7.632e+007	2.544e+007	4.549e+006	0.000
Residual	679996	3.803e+006	5.593		
Total	679999	8.013e+007			

Table 2. One-way ANOVA of zone 1.

In Table 2, the analysis is considered at the significance ($\alpha = 0.05$), so the F value ($F_{0.95;\ 3,\ 679996}$) is 2.6 that is less than F = 4.549e+006. As a result, we refuse H_0 (accept H_a); there is at least one independent variable impacting on the independent variable (T_{S1}). Then, step 3 is further conducted.

In the third step, three assumptions are defined for each selected variable; however, only one (T_{OAT}) is shown as the example:

H_0: T_{OAT} does not influence on a dependent variable (T_{S1}) or $\beta 1 = 0$;

H_1: T_{OAT} influences a dependent variable (T_{S1}) or $\beta 1 \neq 0$

The results of T test and MLR coefficients obtained from statistical toolbox in Matlab are tabulated in Table 3.

Independent variables	Coefficients	T-statistic value	P value
Intercept on Y axis	1.387	154.030	0.000
T_{OAT}	-0.307	-1046.314	0.000
T zone1	1.379	2096.926	0.000
T zone2	-0.157	-200.891	0.000

Table 3. T-statistic values and coefficients with significance of zone 1.

In Table 3, the t-statistic value of the three independent variables (T_{OAT}, T_{Z1} and T_{Z2}), which is obtained from the t distribution table, at $t_{0.975,\ 679996}$ is 0.196 being less than the absolute of the t-statistic values ($|t| > t_{1-\alpha/2;n-k-1}$) of T_{OAT}, T_{Z1}, and T_{Z2}. On the one hand, all p values in Table 3 are 0.00 being less than the significance at $\alpha=0.05$. Therefore, the analysis accepts the alternative hypothesis (H_1). As a result, T_{OAT}, T_{Z1} and T_{Z2} significantly impact on the T_{S1} and can be utilized to construct a MLR equation in next step.

With the statistical results, all coefficients in the second column of Table 3 are utilized to construct MLR as the steady-state model for predicting virtual wall surface temperature in zone 1. The MLR model of zone 1 is:

With the statistical results, all coefficients in the second column of Table 3 are utilized to construct MLR as the steady-state model for predicting virtual wall surface temperature in zone 1. The MLR model of zone 1 is:

$$T_{S1} = -0.307 T_{OAT} + 1.379 T_{Z1} - 0.157 T_{Z2} + 1.387$$

(2)

Following the same procedures of zone 1, the MLR models of zone 2 and 3 are:

$$T_{S2} = -0.341 T_{OAT} + 0.076 T_{Z2} + 1.098 T_{Z3} + 3.702$$

(3)

$$T_{S3} = -0.466 T_{OAT} + 1.889 T_{Z1} - 0.289 T_{Z2} + 0.361$$

(4)

After obtaining equation 2, 3 and 4, the final step is to investigate the assumption of MLR. Normal probability plot and residual plot between each independent variable and residual are used to check the assumptions. In zone 1, the results are illustrated in Figure 17 and 18 in Appendix B.

4. Model validation

After obtaining the suitable and potential MLR equations in last section, the equations are tested by off-control conditions in three zones for two days in July. They will be further validated and compared to the predicted results obtained from the dynamic virtual wall surface temperature sensors proposed by Yu et al., (2014). The validation criteria, G and R^2 are used to validate the performance prediction of the steady-state models via the off-control condition in Figure 4, 5 and 6.

Based on equation 2, 3 and 4, the validation of the models is processed through the two validation criteria:

G: $$G = \left(1 - \sqrt{\frac{\sum_{i=1}^{N}(y_{p,i} - y_i)^2}{\sum_{i=1}^{N}(y_i - \frac{1}{N}\sum_{i=1}^{N}y_i)^2}}\right) \times 100 \quad , for \ \ i = 1,....,N \quad (5)$$

R^2 is the explanatory power of the regression performed in term of R-squared value, computed from the sums-of-squares terms in equation 6.

$$R^2 = \frac{SSR}{SST} = 1 - \frac{SSE}{SST} \quad (6)$$

Where $SSE = \sum_{i=1}^{n}e_i^2$; sum of squares,

error and $SST = \sum_{i=1}^{n}(y_i - \bar{y})^2$; sum of squares,

total $SSR = \sum_{i=1}^{n}(\hat{y}_i - \bar{y})^2$; sum of squares, regression;

in R-squared value, n is a number of samples.

Goodness of fit demonstrates how similar a predicted model is to measured data, while R-square value computes minimum error between predicted and measured values. Thus, with the different methodologies, the result of R-square value criterion is practically higher than the result of G.
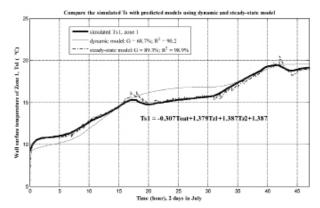
$$R^2 = \frac{SSR}{SST} = 1 - \frac{SSE}{SST} \quad (6)$$

Figure 4. The compared results between dynamic virtual and steady-state virtual sensor in zone 1.
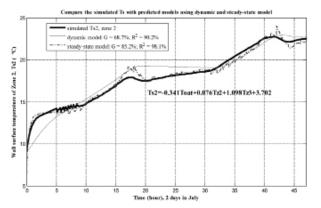

Figure 5. The compared results between dynamic virtual and steady-state virtual sensor in zone 2.

From Figure 4 to Figure 6, the steady-state models as shown in Equation 2, 3 and 4 demonstrate better predicted results than the dynamic models. Utilizing G and R^2 criteria, the G values of the models can be increased from around 69% to 89%, 85% and 87% for zone 1, zone 2 and zone 3, respectively. Additionally, r-square values of the steady-state models can reach to the highest value at around 99% in zone 1.
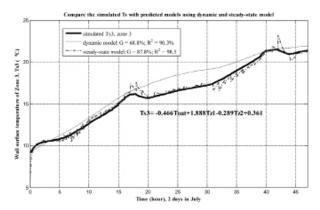
Figure 6. The compared results between dynamic virtual and steady-state virtual sensor in zone 3.
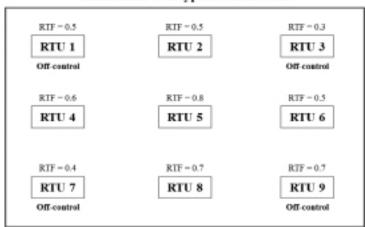

Figure 7. The illustration of a novel control method for 9 RTUs in a typical retail store.

With G criterion, the percentage being more than 85% is very high and robust enough in terms of model prediction because G at 85% refers to a predicted model can track the true value well in any application. Therefore, the steady-state model of the virtual sensor is potentially applied in predicting wall surface temperatures for the off-control conditions since it is appropriate for slow response or a steady-state system.

5. Performance model test via sensitivity analysis

To further test the limited performances of the developed model for applying in a novel supervisory control and for predicting wall surface temperature in other applications such as renewable energy (Niu, Yu & Waradechjumroen, 2014), sensitivity analysis is a powerful tool to further investigate the feasibility of the developed model before embedding or installing in real applications. For the future application, the three on-control conditions including under-sizing, proper-sizing and oversizing conditions can happen in routine operations. The under-sized capacities are decreased 30% from the suitable capacities mentioned in section 2, whereas the oversized capacities are increased 30% from the proper capacity introduced in section 2. Each condition will be used to evaluate the performance of the model in each zone.

5.1 Undersized control
The first test is conducted by the undersized on-off control that seldom occurs in real operations since oversized capacities have been practically designed by HVAC designers; at least 15 to 25% of the actual calculated capacity is over designed to supply adequate cool and heat in the hottest and coldest periods. For example, 40% of surveyed RTUs (Felts & Bailey, 2000) were more than 25% oversized. For our future application, however, the compressors of some zones will be turned off; the off-control zones will be provided cooling or heating by on-control adjacent zones.

To be more specific and clear, Figure 7 demonstrates the operations of 9 RTUs in a typical retail store. With the operations at a peak load condition, 5 RTUs including No. 2, 4, 5, 6 and 8 are continuously turned on, whereas the rest of them are turned off or off-control operation. Using the heat transfer movement, zones that are served by RTU No. 1, 3, 7 and 9 will obtain cooling or heating from the on-control adjacent zones. For example, zone 1 will receive the cooling from zone 2, 4 and 5. As a result, T_{Z1} is not directly control by its thermostat; this example may lead to slow response and is similar to an under-sizing condition of the on-off control.

By following the same procedures as section 4, the under-sizing conditions are simulated for a cooling mode at three peak days in July. The results can be illustrated in Figure 8, 9 and 10 for zone 1, zone and zone 3, respectively. The mode prediction of zone 1 and 3 perform very well (G being more than 85%) except zone 2 since this zone has the higher wall surface temperature fluctuation from 35th hour to 42th hour than other zones when undersized on-control actions are operated. In addition, it is obvious that model prediction degradation happens because there are high error predictions on the last day. With comparing with the dynamic model, the prediction performances are worse than the dynamic model performances; however, MLR models guarantee the prediction at 74% when they are implemented on Simulink.

For this case, it is the main objective of supervisory control to reduce oversized capacities of all RTUs and to manipulate all zones in a proper-sizing condition. Thus, the wall surface temperature will be predicted by the virtual sensor algorithms when the predicted values of the virtual sensor are used as operational constraints for optimization function to optimally compute the supervisory control command. The on-control data is also obtained by the same periods as the undersized control. The predicted steady-state model of each zone is resulted in Figure 11, 12 and 13.

In this condition, the results are similar to the under-sizing conditions. Specifically, zone 2 could be affected by higher RTU capacities resulting in lowest prediction percentage from other zones. All predicted results of the current condition are lower than the under-sizing conditions because increases higher capacities and high fluctuation of wall surface temperature results in performance degradation of the steady-state models in all zones.
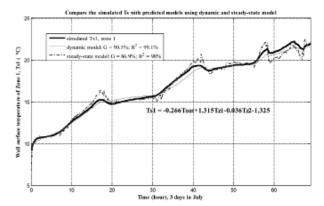
Figure 8. The compared results between dynamic virtual and steady-state virtual sensor via an under-sizing condition in zone 1.
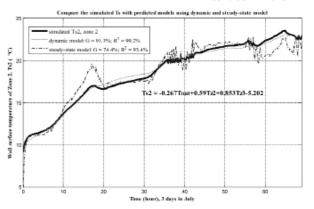
Figure 9. The compared results between dynamic virtual and steady-state virtual sensor via an under-sizing condition in zone 2.
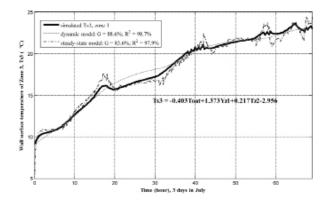
Figure 10. The compared results between dynamic virtual and steady-state virtual sensor via an under-sizing condition in zone 3.
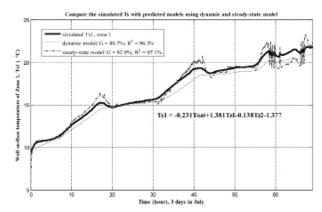
Figure 11. The compared results between dynamic virtual and steady-state virtual sensor via a proper-sizing condition in zone 1.
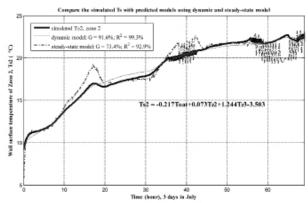

Figure 12. The compared results between dynamic virtual and steady-state virtual sensor via a proper-sizing condition in zone 2.
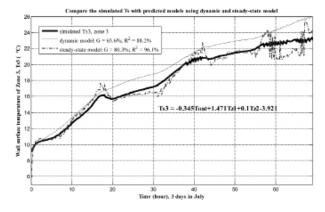

Figure 13. The compared results between dynamic virtual and steady-state virtual sensor via a proper-sizing condition in zone 3.

Based on Figure 11, 12 and 13, there are more on-off cycles at the peak conditions of each day leading to more oscillation of prediction performances. Consequently, the steady-state models perform poor at around peak load of each day (19th hour, 40th hour and 58th hour). In contrast, they still can track the true values well when the periods are out of the on-control actions. This conclusion insists that MLR is suitable for off-control operations of RTUs. Meanwhile, the dynamic model performances are various; they vary from 65% to 90% based on the G values for Simulink implantations. The MLR models guarantee the prediction performance at 73%.

5.3 Oversized control

In contrast to a proper-sizing condition, RTF (runtime fraction) and N (a number of cycles) show oversizing signature that consists of low RTF and high N. This on-control condition practically exists in multi-zone commercial buildings because of several factors. For example, the main results of previous interviews (Djunaedy, Wymelenberg, Acker & Thimmanna, 2011, pp. 468-475) and surveys (Felts & Bailey, 2000) were concluded that a number of designers size RTUs based on over internal load, rules of thumb or related safety factors by software tools leading to oversizing problem. The characteristics of control response perform very fast. As a result, a RTU compressor is frequently cycled since the room temperature meets a set-point temperature before appropriate time. With the theory of on-off control, this control condition will has more compressor cycles than proper-sizing conditions, so the results should be degraded due to more cycles of on-off control at peak load resulting in lower overall performance.
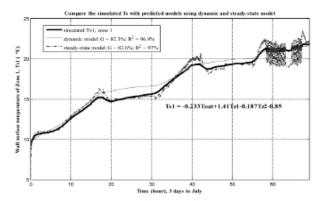
Figure 14. The compared results between dynamic virtual and steady-state virtual sensor via an oversizing condition in zone 1.
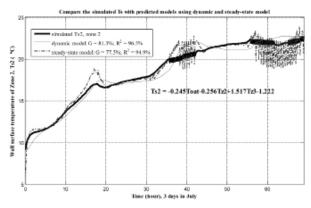

Figure 15. The compared results between dynamic virtual and steady-state virtual sensor via an oversizing condition in zone 2.
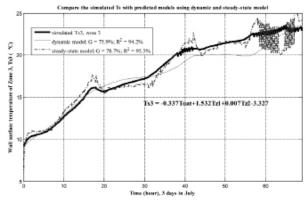

Figure 16. The compared results between dynamic virtual and steady-state virtual sensor via an oversizing condition in zone 3.

Based on the demonstrations of Figure 14 and 16, the results of zone 1 and 3 are lower than other on-control cases since there are more cycles at the peak load condition of each day. However, zone 2 performs better than others. In Figure 15, on the other hand, zone 2 performs better than others because the residuals are more constant than others causing a little higher prediction percentage than other control cases. The lowest performance prediction is 77% based on G criterion.

6. Conclusions

This study improves the prediction performance of dynamic virtual wall surface temperature by proposing the steady-state wall surface temperature which systematically utilizes the application of MLR. With the validation via high G and R^2 values, the predicted models demonstrate excellent results for the off-control condition. Their performances of the dynamic models are improved about 16-20% based on the G criterion. With this validation, the proposed steady-state virtual sensor can be utilized to improve the prediction performance of the dynamic virtual sensor for off-control conditions.

To further evaluate the performance of the model, sensitivity analysis is used to investigate the feasible results under three on-control conditions. The factor degrading prediction performances can be concluded as follows:

1) The performance of the steady-state model will be degraded when the true values are strongly affected by frequently on-off cycles at peak load conditions impacting on overall performance.
2) Since MLR is based on the assumption (constant standardized residual), a selected steady-state model will perform in prediction well if the standardized residuals are approximated to be near-zero.

With faster system response of the on-control actions, the proposed steady-state model is more appropriately applied to detect faulty wall surface temperature prediction for on-control conditions since the results are definably better than 70% based on G criterion. The dynamic model almost performs better than the steady-state model under on-control conditions. However, for slow system response, the proposed model can be embedded into a supervisory control for a future research for predicting slow system response occurring in off-control zones. Also, the proposed virtual sensor can be utilized to predict wall surface temperature for the applications of cooling and heating wall in commercial buildings in renewable energy areas.

Appendix:

Appendix A

Description	Unit	Value	Comments
Volume zone 1	m³	525	
Heat gain for 4 persons	W	600	150 W / person
Heat gain 1 computers	W	500	
Lighting, etc.	W	600	
Moisture production for 4 persons	kg/s	11.0E-05	5.5E-0.5 per 2 persons
Moisture production plant	kg/s	5.8E-06	
Volume zone 2	m³	525	
Heat gain for 4 persons	W	600	150 W / person
Lighting, etc.	W	600	
Moisture production for 4 persons	kg/s	11.0E-05	5.5E-0.5 per 2 persons
Moisture production plant	kg/s	5.8E-06	
Volume zone 3	m³	1050	
Heat gain 8 person	W	900	150 W / person
Moisture production for 8 persons	kg/s	22.0E-05	5.5E-0.5 per 2 persons
Lighting, etc.	W	600	

Table 4. Properties of the three zones for input parameters in simulation.

Description	Unit	Value	Comments
External wall north [EW_N]	m²	105	Limestone, insulation, air gap, brick
Glazing	m²	7.5	HR + glass double glazing
Orientation		90, 180	
External wall east [EW_E]	m²	70.0	Limestone, insulation, air gap, brick
Glazing zone 2	m²	2.4	HR + glass double glazing
Glazing zone 3	m²	4.8	Single glazing
Orientation		90, 270	
External wall east [EW_S]	m²	105.0	Limestone, insulation, air gap, brick
Orientation		90, 0	
External wall east [EW_W]	m²	70	Limestone, insulation, air gap, brick
Glazing zone 1	m²	3.0	HR + glass double glazing
Glazing zone 3	m²	4.8	Single glazing
Orientation		90, 90	
Floor construction	m²	600	Covering, concrete (Assume adiabatic)
Orientation		0, 0	
Roof construction	m²	600	Plaster, air gap, concrete, insulation, PVC
Orientation		0, 0	

Table 5. Properties of the building construction for simulation platform.
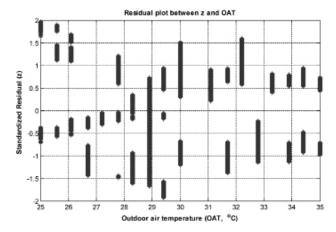
Figure 17. The example of the residual plot between standardized residual and OAT.
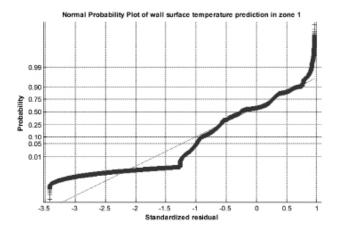

Figure 18. Normal probability plot of error predictions in zone 1.

Appendix B

In this section, the two figures provide the investigation of MLR assumptions that includes: 1) constant standardized residual and 2) the error distribution is under normal curve. In Figure 17, it is the example of residual plots between standardized and OAT. We can notice that the residuals are located around zero that supports the first assumption.

In Figure 18, this is a normal probability plot of the errors between the predicted wall surface temperatures and the simulated values via off-control condition in zone 1. The dash line can be approximated to be the average line for the plus symbols. It demonstrates that the error distributions are normal curve supporting the second assumption.

Appendix C

Virtual surface temperature is based a heat balance equation (Yu, Woradechjumroen & Yu, 2014) The dynamic model of this virtual sensor is initially derived from the heat balance equation at a virtual wall surface in equation 7. The two major assumptions used in Figure 19 include: 1) each zone is well mixed and 2) heat radiation exchanges between a zone and surfaces are neglect. With these simplifications, the heat balance equation of the virtual surface temperature consists of three load components: heat flow through overall building components; heat flow from the current zone; and heat flow from adjacent zones. Therefore, the heat balance model at the virtual wall can be model:

$$\dot{m}_i(C_{pa})\frac{d}{dt}\left(T_{s_i}\right) = h_i A(T_i - T_{s_i}) + \sum_{j \in N_i} h_j A(T_j - T_{s_i}) + \frac{(T_{OAT} - T_{s_i})}{R_{ToT_i}} \quad (7)$$

where i is zone index; j is adjacent zone index; C_{pa} is the specific heat capacity of dry air; T_i , T_{s_i} and T_{OAT} are room temperature , surface temperature in zone i and outdoor air temperature ; m_i is the mass of a virtual wall; h_i and h_j are convective heat transfer coefficients of a room temperature and adjacent zone and R_{ToT_i} is total thermal resistance of external walls, windows and roof.

Using a weight version of the central difference approximation as shown in equation 8,

$$\frac{d}{dt}T_s \approx k_1\left(\frac{T_{s,n+1}-T_{s,n}}{\Delta t}\right) + k_2\left(\frac{T_{s,n}-T_{s,n-1}}{\Delta t}\right); k_1 + k_2 = 1 \quad (8)$$

The physical model can be arranged in the form of the linear parametric model in equation 9 for real-time programming. The arrangement of the physical model based ARX model is:

$$(1+\beta_{i1}q^{-1}+\beta_{i2}q^{-2})T_{S,n} = \alpha_i T_{air,n-1} + \sum_{j\in N_i}\alpha_j T_{S_j,n-1} + \alpha_{OAT}T_{OAT,n-1} \quad (9)$$

in which $\quad \alpha = \dfrac{\Delta t}{m_i C_{pa} k_1}$, $\alpha_i = h_i A\alpha$, $\alpha_{OAT}=\dfrac{\alpha}{R_{ToT_i}}$, $\alpha_j = h_j A\alpha$

and $\beta_{i1}=\dfrac{1-2k_1}{k_1}+\alpha_i+\alpha_{OAT}+\sum_{j\in N_i}\alpha_j$, $\beta_{i2}=\dfrac{k_1-1}{k_1}$
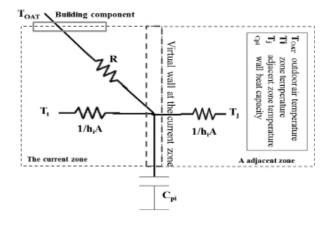

Figure 19. A circuit-equivalent 3R1C of a thermal network for the virtual surface temperature model.

References

Aranda, A., Ferreira, G., Mainar-Toledo, M. D., Scarpellini, S. & Sastresa, E. L. (2012). Multiple regression models to predict the annual energy consumption in the Spanish banking sector. *Energy and Buildings, 49*, 380-387.

Asuero, A. G., Sayago, A. & Gonzalez, A. G. (2006). The correlation coefficient: An overview. *Critical Reviews in Analytical Chemistry, 36*, 41–59.

American Society of Heating, Refrigeration and Air-Conditioning Engineering. (2009). *ASHARE Handbook – Fundamentals*. Atlanta, GA: Author.

Bonne, D. & Jorgensen, S. B. (2004). Data-driven modeling of batch processes. *Proceedings of 7th International Symposium on Advanced Control of Chemical Processes (ADCHEM) January*. Hong Kong, China.

Catalina, T., Virgone, J. & Blanco, E. (2008) Development and validation of regression models to predict monthly heating demand for residential buildings. *Energy and Buildings, 40(*10), 1825–1832.

DOE. (2011). *Energy Information Administration (EIA), Annual Energy Outlook*. USA: Author.

Djunaedy, E., Wymelenberg, K. V. D., Acker, B. & Thimmanna, H. (2011). Oversizing of HVAC system: signatures and penalties. *Energy and Buildings, 43*(2-3), 468-475.

Felts, D. R. & Bailey, P. (2000). The State of Affairs - Pack aged cooling equipment in California. *Proceedings of the 2000 ACEEE summer study on energy efficiency in buildings*. California, Washington, DC.

Hair, L., Anderson, R. E., Tatham, R. L. & Black, W.C. (1995). *Multivariate data analysis (4th ed.)*. New Jersey: Prentice-Hall Inc.

James, S., Legge, R. & Budman, H. (2002). Comparative study of black-box and hybrid estimation methods in fed-batch fermentation. *Journal of Process Control, 12*(1),113–121.

Katipamula, S., Reddy, T. A. & Claridege, D. E. (1998). Multi variate regression modeling. Journal of Solar *Energy Engineering, 120*(3), 177-184.

Lam, J. C., Wan, K. K. W, Liu, D. & Tsang, C. L. (2010). Multiple regression models for energy use in air-conditioned office buildings in different climates. *Energy Conversion and Management, 51*(12), 2692–2697.

Li, H. & Braun, J. E. (2007a). Decoupling features and virtual sensors for diagnosis of faults in vapor compression air conditioners. *International Jounal of Refrigeration, 30*(3), 546-564.

Li, H. & Braun J. E. (2007b). A methodology for diagnosing multiple-simultaneous faults in vapor compression air conditioners. *HVAC&Research, 13*(2), 369–395.

Li, H., Yu, D. & Braun, J. E. (2011). A review of virtual sensing technology and application in building system. *HVAC&R Research, 17*(5), 619–645.

Niu, F., Yu, Y. & Woradechjumroen, D. (2014). Investigation of an active tuning building envelop based on capillary network. *International Conference on Sustainable Design, Engineering and Construction (ICSDEC)*, China.

Reddy, T. A. (2006). *Evaluation and assessment of fault detection and diagnostic methods for centrifugal chillers—Phase II.: GA Final project report of ASHRAE Research Project RP-1275, June*. GA: Atlanta.

Rivers, N. (n.d.). *Management of energy usage in supermar ket refrigeration systems (Session 2004-2005)*. Carshalton, Surrey: The Institute of Refrigeration.

Schijndel, A. W. M. van (2007). *Integrated heat air and moisture modeling and simulation*. Eindhoven: Technische University Eindhoven.

Woradechjumroen, D., Yu, Y., Li, H., Yang, H. & Yu, D. (2014). Analysis of HVAC system oversizing in commercial buildings through field measurements. *Energy and Buildings, 69*, 131–143.

Wilcox, S. & Mario, W. (2008). *Users manual for TMY 3 data sets (Technical Report NREL TP–581-4356, May 2008)*. Colorado: National Renewable Energy Laboratory.

Yang, H., Xu, Z., Xiong, R., Li, H., Zhang, T.C., Liu, X. & Woradechjumroen, D. (2014). Simplifying manu facturers' data in unitary HVAC equipment through a DX cooling coil modeling. *Energy and Buildings 74*, 152-162.

Yu, Y., Woradechjumroen, D. & Yu, D. (2014). Virtual surface temperature sensor for multi-zone commercial buildings. *The 6th International Conference on Applied Energy, Taipei City*. Taiwan, China.